Progress In Electromagnetics Research, PIER 101, 97–114, 2010

CLOSED-FORM DESIGN METHOD OF AN N-WAY DUAL-BAND WILKINSON HYBRID POWER DIVIDER

Y. L. Wu, Y. A. Liu, S. L. Li, C. P. Yu, and X. Liu

School of Electronic Engineering
Beijing University of Posts and Telecommunications
China

Abstract—In this paper, the closed-form design method of an N-way dual-band Wilkinson hybrid power divider is proposed. This symmetric structure including N groups of two sections of transmission lines and two isolated resistors is described which can split a signal into N equiphase equiamplitude parts at two arbitrary frequencies (dual-band) simultaneously, where N can be odd or even. Based on the rigorous even- and odd-mode analysis, the closed-form design equations are derived. For verification, various numerical examples are designed, calculated and compared while two practical examples including two ways and three ways dual-band microstrip power dividers are fabricated and measured. It is very interesting that this generalized power divider with analytical design equations can be designed for wideband applications when the frequency-ratio is relatively small. In addition, it is found that the conventional N-way hybrid Wilkinson power divider for single-band applications is a special case (the frequency-ratio equals to 3) of this generalized power divider.

1. INTRODUCTION

In microwave and millimeter-wave circuits, power dividers are widely used as key passive components. As is well known, the first complete design method for N-way power dividers was developed by Wilkinson [1] in 1960. And then, the appearance of Wilkinson power dividers has lead to further researches on bandwidth enhancement [2] and planar circuit's applications [3, 4] of N-way power dividers. In addition, extending from equal and symmetric N-way power dividers,

Corresponding author: Y. L. Wu (wuyongle138@gmail.com).

general design equations of N-way power dividers with arbitrary power dividing ratios were presented in [5]. Recently, novel N-way microwave power dividers are developed based on meta-materials in [6, 7] while full-wave analysis of N-way power dividers by eigenvalue decomposition is reported in [8]. However, these N-way power dividers discussed in [1–8] and unequal lumped-elements power dividers analyzed in [9] are proposed only for single-band (or wideband) applications. To satisfy dual-band or multi-band applications, novel dual-band transformers [10–13], equal dual-band power dividers [14–24], and unequal dual-band modified power dividers [25–30] with closed-form design equations are developed. Although the power dividers presented in [14–30] can operate at two bands, only two-way structures are considered. As the extension of the three-way single-band power divider in [3], the paper [31] introduces a planar three-way dual-frequency power divider, however, the design method is only considered for this special three-way case. More recently, the concept of N-way dual-frequency power dividers is discussed and the corresponding numerical design method is based on genetic algorithm [32]. In addition, the developments of new Wilkinson power dividers with small size [33, 34], harmonic suppression [35] or 6 : 1 unequal power division [36] are new research topics.

In this paper, we analyze a generalized equal Wilkinson hybrid power divider, which includes N-way and can operate at two arbitrary frequencies (dual-band) simultaneously, namely, a multi-way dual-band power divider. The analyzed structure consists of N groups of two-section transmission lines and two isolated resistors, which is similar with the design structure in [32]. Different from the design method of [32], the values of design parameters in this paper can be calculated by closed-form design equations, in other words, the design method of the N-way dual-band power divider is *analytical*. In this generalized power divider, there are two important characteristics. One is that it can be used in wideband applications when the frequency-ratio (the center frequency-ratio of dual-band) is relatively small (for example, it is smaller than two). The other is that the analyzed N-way dual-band Wilkinson hybrid power divider is an extension of the N-way single-band power divider developed by Wilkinson [1] when the frequency-ratio v equals to three.

2. CIRCUIT STRUCTURES AND DESIGN EQUATIONS

Figure 1 illustrates the basic circuit structure of the analyzed N-way dual-band Wilkinson hybrid power divider. As shown in Fig. 1, the total structure includes N groups of two-section of transmission lines

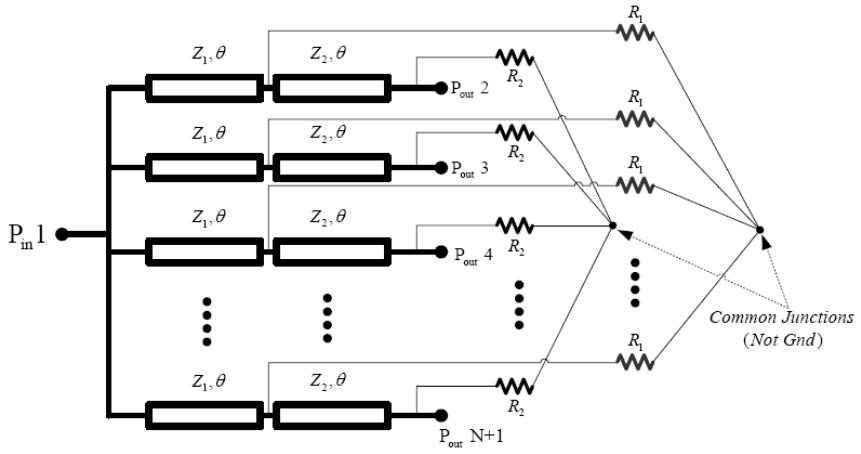

Figure 1. The analyzed circuit of N-way dual-band Wilkinson hybrid power divider.

(Z_1 and Z_2) with the same electrical length θ and two isolated resistors (R_1 and R_2). N symmetric parallel dual-frequency transformers [10] can achieve the ideal input matching at the input Port 1. At the output ports (such as Port 2, ..., $(N+1)$ in Fig. 1), the ideal output matching and isolation between two arbitrary output ports can be obtained by N groups of two separated isolated resistors R_1 and R_2. In particular, when N equals to two, this generalized power divider can be simplified to a new kind of two-way dual-band power divider with bandwidth enhancement [24]. Actually, this simple case, which will be discussed in section 4, is very suitable for distributed circuit implementation. When the value of N is larger than three, the planar circuit implementation becomes difficult. Therefore, the three-dimensional (3D) structure including splines and coaxial lines [1] should be used to implement dual-band Wilkinson hybrid power divider with N ($N > 3$) output ports. The analytical design equations can be derived with the aid of the conventional even- and odd-mode analysis [14], and the complete process is given in the rest of this chapter.

2.1. The Even-mode Analysis

In even-mode analysis, Fig. 1 is simplified to Fig. 2. From Fig. 2, to match the input Port 1, the value of input equivalent impedance on arbitrary way $n \in \{2, 3, \ldots, (N+1)\}$ should be calculated by

$$Z_{in}|_n = NZ_0, \tag{1}$$

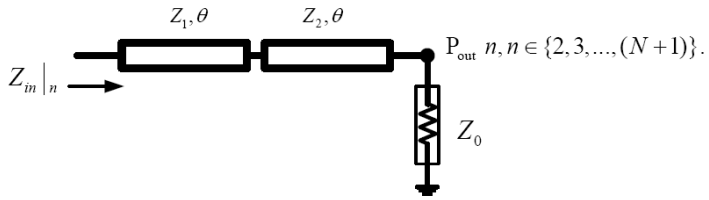

Figure 2. The equivalent circuit of N-way dual-band Wilkinson hybrid power divider for the even-mode analysis.

where N is the number of transmission ways and Z_0 is the internal equivalent impedance at each port. For convenience, the center frequencies of two designated bands are defined as

$$f_1, f_2 = v f_1, \tag{2}$$

where v is the frequency-ratio and the value of v satisfies $v \geq 1$. Using the analytical method of two-section transformer given in [10], the final design equations for electrical parameters of each section transmission line can be expressed as

$$\theta = \frac{m\pi}{1+v}, \text{at } f_1, \ m \in \{1, 2, \ldots\}, \tag{3}$$

$$p = \tan^2(\theta), \tag{4}$$

$$Z_1 = \sqrt{N} Z_0 \sqrt{\frac{1-N}{2p} + \sqrt{\left(\frac{1-N}{2p}\right)^2 + N}}, \tag{5}$$

$$Z_2 = \frac{N Z_0^2}{Z_1} = Z_0 \sqrt{\frac{N-1}{2p} + \sqrt{\left(\frac{N-1}{2p}\right)^2 + N}}. \tag{6}$$

Therefore, once the values of N and v are known in practical design circuits, the electrical parameters can be calculated using (3)–(6) analytically. To determine the values of isolated resistors, it is necessary to apply the odd-mode analysis, which will be discussed in the following subsection.

2.2. The Odd-mode Analysis

In odd-mode analysis, Fig. 1 is equivalent to Fig. 3. To obtain the ideal isolation and matching at all of output ports in Fig. 1 and Fig. 3, the mathematical relationship between isolated resistors and electrical

parameters of transmission lines can be written as

$$Z_{Temp} = \frac{jZ_1R_1\tan(\theta)}{jZ_1\tan(\theta)+R_1}, \tag{7}$$

$$\frac{1}{Z_0} = \frac{Z_2+jZ_{Temp}\tan(\theta)}{Z_2[Z_{Temp}+jZ_2\tan(\theta)]}+\frac{1}{R_2}, \tag{8}$$

where Z_{Temp} is the internal input impedance shown in Fig. 3. After combining (7) with (8) and separating the real and imaginary part, we can obtain the following equations:

$$\left(\frac{1}{Z_0}-\frac{1}{R_2}\right)Z_1Z_2^2\tan^2(\theta) = R_1[Z_1\tan^2(\theta)-Z_2], \tag{9}$$

$$\left(\frac{1}{Z_0}-\frac{1}{R_2}\right)R_1(Z_1+Z_2) = Z_1. \tag{10}$$

Solving (9) and (10) simultaneously, the final analytical solutions of isolated resistors are obtained as follows (The Equation (4) is used.),

$$R_1 = \sqrt{\frac{Z_1^2Z_2^2p}{(Z_1+Z_2)(Z_1p-Z_2)}}, \tag{11}$$

$$R_2 = \frac{Z_0Z_2\sqrt{p(Z_1+Z_2)}}{Z_2\sqrt{p(Z_1+Z_2)}-Z_0\sqrt{pZ_1-Z_2}}. \tag{12}$$

Obviously, according to (3)–(6), (11) and (12), the values of electrical parameters of transmission lines, isolated resistors R_1 and R_2 can be calculated directly. Consequently, when the first frequency f_1, the frequency-ratio v, and the number of ways N are fixed, based on the structure shown in Fig. 1 and the above closed-form design equations, this generalized and flexible N-way dual-band power divider can be designed easily. Additionally, the implemented structures of this N-way dual-band power divider depend on special technologies, such as microstrip, strip-line, spline, coaxial cable, etc.

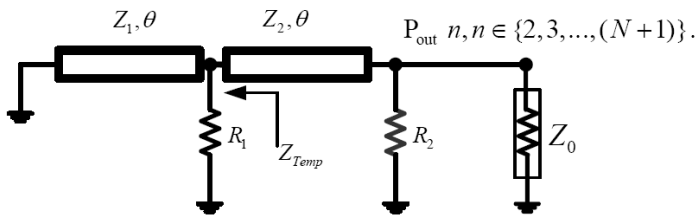

Figure 3. The equivalent circuit of N-way dual-band Wilkinson hybrid power divider for the odd-mode analysis.

2.3. The Available Scope of the Frequency-ratio for Real and Positive Resistors

Here, the available scope of the frequency-ratio in this generalized N-way dual-band power divider is discussed. To assure that the values of isolated resistors R_1 and R_2 are real and positive, from (11) and (12), the following condition should be satisfied simultaneously:

$$Z_1 \tan^2(\theta) - Z_2 \geq 0, \tag{13}$$

$$Z_2\sqrt{\tan^2(\theta)(Z_1+Z_2)} - Z_0\sqrt{Z_1\tan^2(\theta) - Z_2} \geq 0. \tag{14}$$

Substituting (5) and (6) into (13) and (14) at the same time, the constraint situation can be rewritten and simplified as,

$$p^2 \geq 1, \tag{15}$$

$$\frac{N-1}{2p} \geq -\sqrt{\left(\frac{N-1}{2p}\right)^2 + N}. \tag{16}$$

Because $N > 1$, the inequality (16) will be satisfied unconditionally. Therefore, the final constraint condition is only inequality (15). To begin with, $\tan(\theta) > 0$ is considered. Thus, using (3) and (4), the accurate condition $\tan(\theta) > 1$ is obtained and the corresponding condition including initial parameters (such as the frequency-ratio v and the defined positive integer m) can be expressed as

$$k + \frac{1}{4} \leq \frac{m}{1+v} < \frac{1}{2} + k,\ k \in \{0, 1, 2, \ldots\}. \tag{17}$$

And then, $\tan(\theta) < 0$ is considered. Obviously, the values of (11) and (12) must be real and positive when the inequality (15) is satisfied. Similarly, $\tan(\theta) < -1$ can be obtained directly and the corresponding condition is written as

$$k + \frac{1}{2} < \frac{m}{1+v} \leq \frac{3}{4} + k,\ k \in \{0, 1, 2, \ldots\}. \tag{18}$$

After analyzing the internal and special case that $m/(1+v) = 0.5$ (The simplified results of this case are $Z_1 = \sqrt{N\sqrt{N}}Z_0$, $Z_2 = \sqrt{\sqrt{N}}Z_0$, $R_1 = \sqrt{N}Z_0/(\sqrt{1+\sqrt{N}})$, $R_2 = \sqrt{1+\sqrt{N}}(\sqrt{1+\sqrt{N}}+1)Z_0/\sqrt{N}$.) and combining (17) and (18), the final total situation can be summarized as

$$k + \frac{1}{4} \leq \frac{m}{1+v} \leq \frac{3}{4} + k,\ k \in \{0, 1, 2, \ldots\}. \tag{19}$$

Therefore, once the values of m and v satisfy the inequality (19), all of the final design parameters are real and positive. Thus, the design procedure will be practical.

2.4. Design Charts for Normalized Characteristic Impedances of Transmission Lines and Resistors

When the values of N and port impedance Z_0 change, the values of characteristic impedances of transmission lines and isolated resistors will change accordingly. For convenience in designing common multi-way dual-band power dividers, Fig. 4 and Fig. 5 give the design charts for normalized characteristic impedances and resistors. The mathematical definitions of normalized parameters are as follows: $z_1 = Z_1/Z_0$, $z_2 = Z_2/Z_0$, $r_1 = R_1/Z_0$, and $r_2 = R_2/Z_0$. In addition,

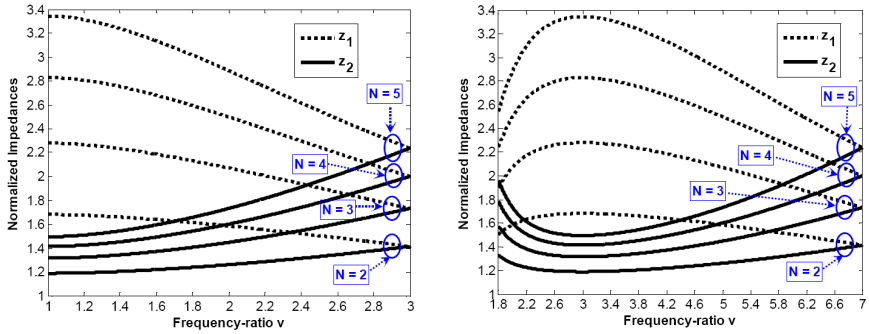

Figure 4. The normalized characteristic impedances (z_1 and z_2) against the frequency-ratio v for various values of N when (a) $m = 1$, and (b) $m = 2$.

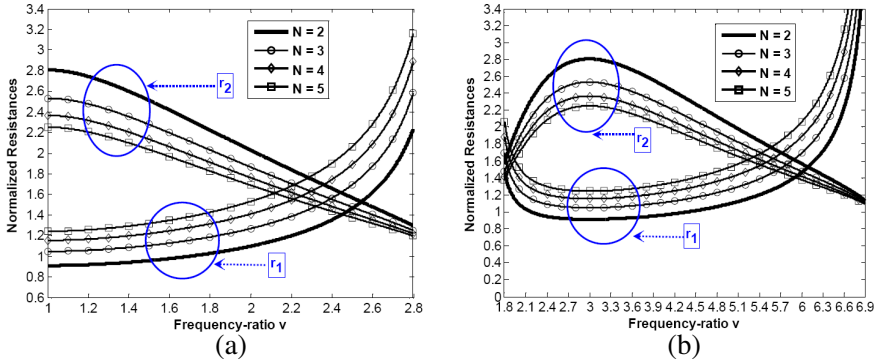

Figure 5. The normalized resistances (r_1 and r_2) against the frequency-ratio v for various values of N when (a) $m = 1$, and (b) $m = 2$.

as shown in both Fig. 4(a) and Fig. 4(b), the larger the N value is, the larger the corresponding values of normalized characteristic impedances are. The value of z_1 decreases as v is increased from 1 to 3 while the value of z_2 increases as v is increased from 1 to 3 in Fig. 4(a). Note that the monotonic properties cannot be observed from Fig. 4(b) when $m = 2$ is adopted. Fig. 5(a) and Fig. 5(b) plot, respectively, the normalized resistances of two isolated resistors with $m = 1$ and $m = 2$ when $N = 2, 3, 4, 5$ are considered. Fortunately, the values of isolated resistors are in the available range of practical lumped-elements when the standard 50-Ω transmission line is used.

2.5. Special Case of the Generalized N-way Dual-band Power Divider

A special case is discussed in this subsection. When $v = 3$ and $m = 1$, $\tan(\theta) = 1$ can be obtained. Thus, from (5), (6), (11) and (12), the following simplest results can be obtained:

$$Z_1 = Z_2 = \sqrt{N} Z_0, \tag{20}$$

$$R_1 = +\infty, R_2 = Z_0. \tag{21}$$

Actually, the Equations (20) and (21) are the same with the results given in [1]. In other words, this paper can be considered as the extension of the N-way single-band power divider developed by Wilkinson in 1960.

3. NUMERICAL EXAMPLES

For theoretical verification, twelve examples are designed using the closed-form design equations (3)–(6), (11), and (12). Numerical results of these examples are based on the lossless transmission line and ideal resistor models. The power dividers with different ways are presented below in details.

3.1. Two-way Dual-band Power Dividers

In two-way dual-band power dividers, four cases (Case 1–Case 4) with different frequency-ratios are designed and the detailed design parameters are listed in Table 1. The amplitude responses of S-parameters over different frequency ranges are shown in Fig. 6. Obviously, ideal return loss of each port and isolation between output ports are attained with insertion loss of 3 dB at two desired frequencies simultaneously in these four cases.

Table 1. Final parameters of four cases in two-way dual-band power divider.

	$f_1 = 1\,\text{GHz}$, $Z_0 = 50\,\Omega$, $N = 2$.			
	Case 1	**Case 2**	**Case 3**	**Case 4**
	$v = 1.4$	$v = 2$	$v = 2.4$	$v = 4$
	$m = 1$	$m = 1$	$m = 1$	$m = 2$
$\theta(rad)_{f_1}$	1.3090	1.0472	**0.9240**	1.2566
$Z_1(\Omega)$	83.0292	79.2885	**76.0768**	82.5352
$Z_2(\Omega)$	60.2198	63.0608	**65.7231**	60.5802
$R_1(\Omega)$	47.0892	54.9005	**67.5861**	47.8985
$R_2(\Omega)$	130.0199	101.4777	**82.9060**	125.6302

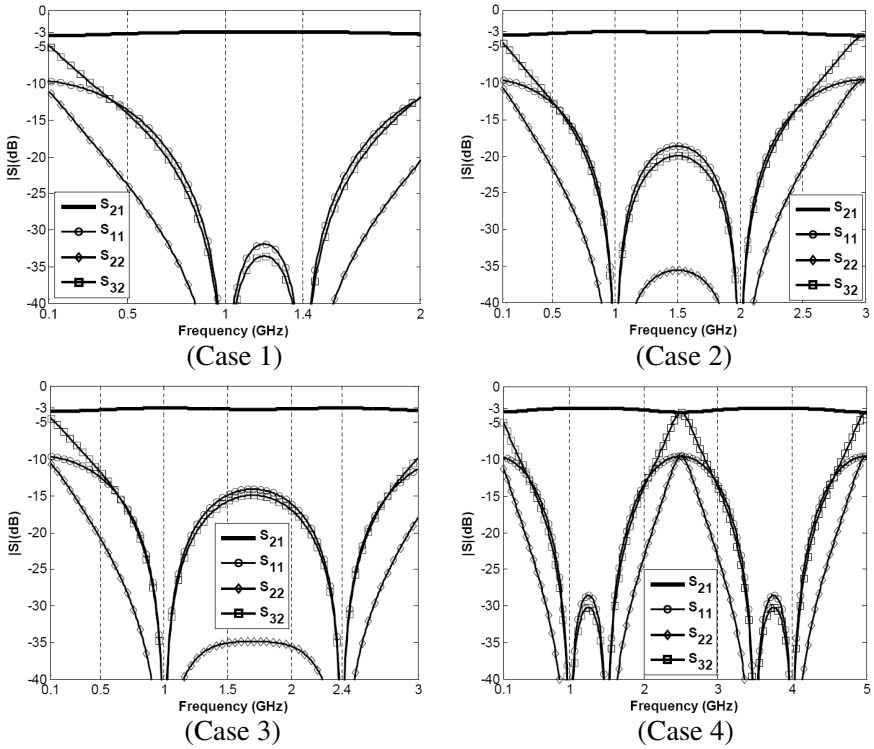

Figure 6. The amplitude responses of S-parameters of Case 1–Case 4 in two-way dual-band power dividers.

Table 2. Final parameters of four cases in three-way dual-band power divider.

	$f_1 = 1\,\text{GHz},\ Z_0 = 50\,\Omega,\ N = 3.$			
	Case 5	**Case 6**	**Case 7**	**Case 8**
	$v = 1.4$	$v = 2$	$v = 2.4$	$v = 4$
	$m = 1$	$m = 1$	$m = 1$	$m = 2$
$\theta(rad)_{f_1}$	1.3090	**1.0472**	0.9240	1.2566
$Z_1(\Omega)$	111.6381	**103.5797**	96.9501	110.5563
$Z_2(\Omega)$	67.1814	**72.4080**	77.3594	67.8387
$R_1(\Omega)$	54.2673	**63.4294**	78.1527	55.2232
$R_2(\Omega)$	117.7062	**93.2750**	77.6203	113.9242

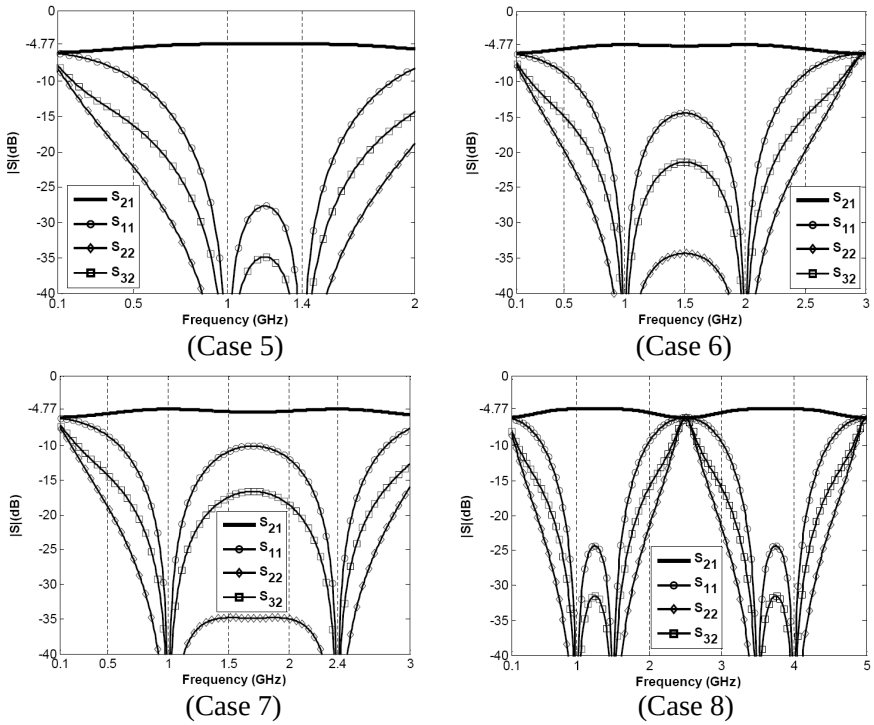

Figure 7. The amplitude responses of S-parameters of Case 5–Case 8 in three-way dual-band power dividers.

Table 3. Final parameters of four cases in four-way dual-band power divider.

	$f_1 = 1\,\text{GHz},\ Z_0 = 50\,\Omega,\ N = 4.$			
	Case 9	**Case 10**	**Case 11**	**Case 12**
	$v = 1.4$	$v = 2$	$v = 2.4$	$v = 4$
	$m = 1$	$m = 1$	$m = 1$	$m = 2$
$\theta(rad)_{f_1}$	1.3090	1.0472	0.9240	1.2566
$Z_1(\Omega)$	137.6663	124.9621	114.8844	135.9375
$Z_2(\Omega)$	72.6394	80.0243	87.0440	73.5632
$R_1(\Omega)$	59.9165	70.4512	87.1217	61.0256
$R_2(\Omega)$	110.1954	88.1287	74.2411	106.7539

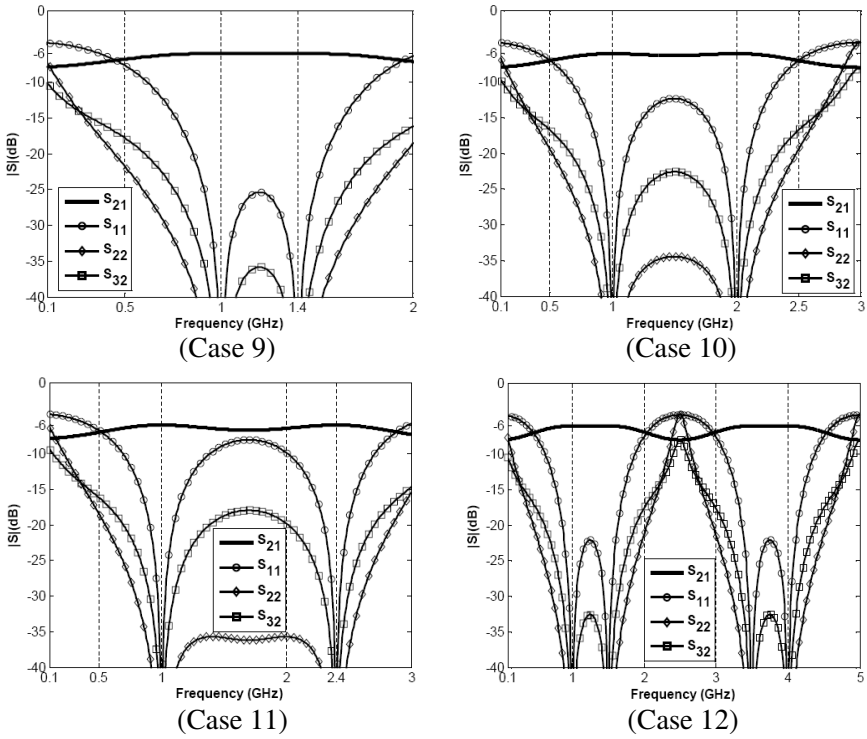

Figure 8. The amplitude responses of S-parameters of Case 9–Case 12 in four-way dual-band power dividers.

3.2. Three-way Dual-band Power Dividers

Similarly, in three-way dual-band power dividers, four cases (Case 5–Case 8) with different frequency-ratios are designed and the detailed design parameters are listed in Table 2. The amplitude responses of S-parameters over different frequency ranges are shown in Fig. 7. In these cases, ideal matching of each port, isolation between output ports, and insertion loss of 4.77 dB are satisfied at two desired frequencies simultaneously.

3.3. Four-way Dual-band Power Dividers

Finally, in four-way dual-band power dividers, four cases (Case 9–Case 12) with different frequency-ratios are designed and the detailed design parameters are listed in Table 3. The amplitude responses of S-parameters over different frequency ranges are shown in Fig. 8. As illustrated in Fig. 8, the matching of both the input port 1 and output ports at two frequencies is ideal, isolation between output ports at two frequencies is perfect, and the insertion loss equals to 6 dB at two desired frequencies simultaneously.

It is necessary to point out that the values of transmission parameters $S_{i1,i=\{2,3,\ldots\}}$, isolation parameters $S_{ij,i=\{2,3,\ldots\},j=\{2,3,\ldots\},i\neq j}$, and output matching $S_{ii,i=\{2,3,\ldots\}}$ maintain the same when locations of ports change in these ideal calculations. Therefore, Fig. 6, Fig. 7, and Fig. 8 only show four different S-parameters including S_{21}, S_{11}, S_{22}, and S_{32}. In addition, when the frequency-ratio is relatively small, these generalized power dividers can be used as wideband ones with N-way, such as Case 1, Case 5, and Case 9. It can be also observed from Case 4, Case 8, and Case 12 that these power dividers have two separated bands with bandwidth enhancement.

4. MICROSTRIP EXAMPLES

In this section, for experimental verification, a two-way power divider operating at 1 GHz and 2.4 GHz and a three-way power divider operating at 1 GHz and 2 GHz are fabricated in microstrip technology. The design parameters are obtained from Case 3 in Table 1 and Case 6 in Table 2, which is given in Section 3. In these two examples, the F4B substrate with a dielectric constant of 2.65 and a thickness of 0.8 mm is chosen. Photographs of the two-way fabricated power divider and the three-way one are shown in Fig. 9 and Fig. 10, respectively. In addition, the area sizes of the two-way fabricated power divider and the three-way one are $71 \times 36\,\text{mm}^2$ and $86 \times 44\,\text{mm}^2$, respectively. All

Figure 9. Photograph of the two-way dual-band fabricated power divider (Case 3).

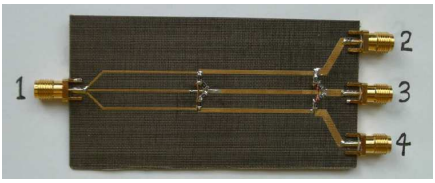

Figure 10. Photograph of the three-way dual-band fabricated power divider (Case 6).

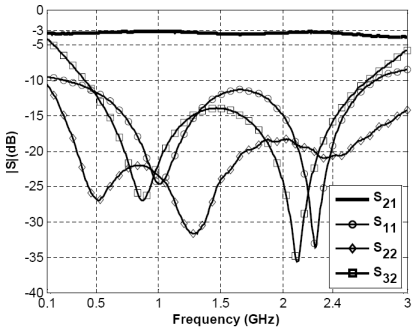

(a)

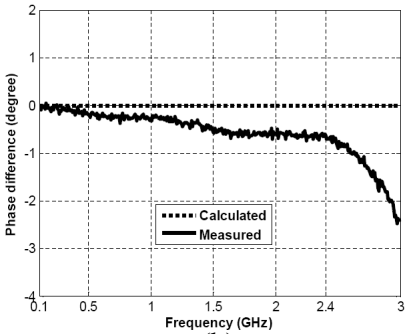

(b)

Figure 11. The measured S-parameters of the two-way dual-band power divider (Case 3): (a) Magnitude; (b) Phase difference including calculated results (Ang (S_{31})–Ang (S_{21})).

the measured results shown in Fig. 11 and Fig. 12 are collected from Agilent N5230C network analyzer.

From Fig. 11(a), in this microstrip two-way dual-band power divider, the absolute value of transmission parameters $S_{21}(S_{21} \cong S_{31})$ is approximately -3.1 dB while all of the input and output ports matching and isolation are below -15 dB at both 1 GHz and 2.4 GHz. As shown in Fig. 11(b), the phase difference between the output port 3 and the output port 2 is in the range of $\pm 0.8°$ at both 1 GHz and 2.4 GHz. Therefore, according to calculated results shown in Fig. 6 (Case 3), there is a good agreement between our design goals and practical measurements.

In the microstrip three-way dual-band power divider, as shown in Fig. 12(a), all of the input matching $|S_{11}|$ and the output matching including $|S_{22}|$, $|S_{33}|$, and $|S_{44}|$ are below -15 dB at both 1 GHz and 2 GHz. From Fig. 12(b), all of measured transmission parameters $|S_{21}|$,

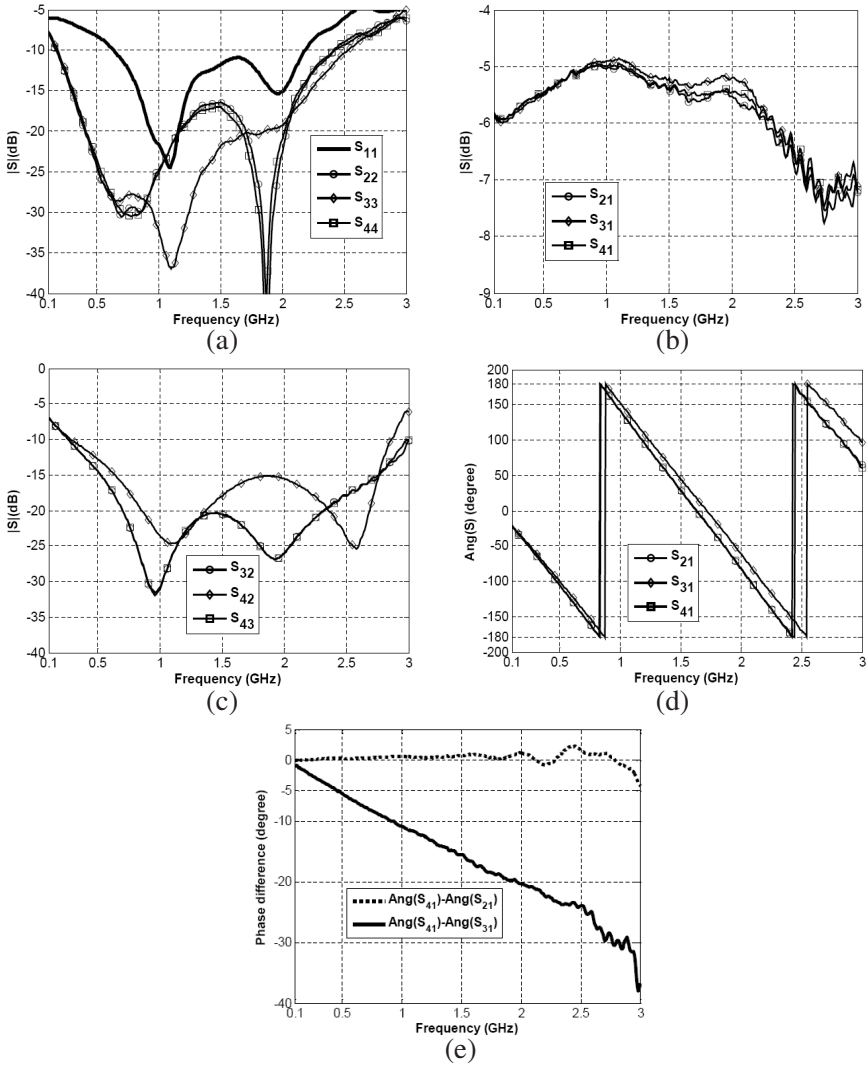

Figure 12. The measured S-parameters of the three-way dual-band fabricated power divider (Case 6): (a) Matching; (b) Transmission (Magnitude); (c) Isolation; (d) Transmission (Phase); (e) Transmission (Phase difference).

$|S_{31}|$ and $|S_{41}|$ are approximately equal and the corresponding values are in the range of -4.9 dB to -5.0 dB at 1 GHz and -5.2 dB to -5.5 dB at 2 GHz. The good isolation between the output ports (such as the port 2, 3, and 4) can be observed from Fig. 12(c). Moreover, the phase information is shown in Fig. 12(d) and Fig. 12(e). The electrical length

at the port 3 is shorter than other output ports in actual circuit shown in Fig. 10, thus, it is indicated in Fig. 12(e) that the phase difference between the port 4 and the port 3 decreases linearly as the operating frequency increases. Meanwhile, because path electrical lengths at the port 2 and the port 4 are equal, the phase difference between these two output ports is in the range of $\pm 1.2^\circ$ at 1 GHz and 2 GHz. In fact, a few disagreements between calculation and measurement may be caused by the loss characteristic of the substrate and two jumper wires connecting isolated resistors as the common junctions in this planar structure (shown in Fig. 10). In a word, the measurements of this three-way fabricated power divider operating at 1 GHz and 2 GHz can satisfy the requirement of common dual-band systems.

In summary, there are good agreements between the measured results and the desired performances in these two microstrip examples, in other words, these examples effectively verify the analytical approach for the generalized N-way dual-band power divider as typical samples. Furthermore, the four or more ways dual-band power dividers are not suitable for planar implementations, thus, a three-dimensional structure including splines and coaxial lines should be applied like the original Wilkinson power divider [1].

5. CONCLUSIONS

An N-way Wilkinson dual-band power divider with simple structure and without reactive components is analyzed in this paper. The final analytical (closed-form) design equations are obtained and the design charts of normalized parameters are given. The generalized structure and analytical design method are verified by twelve numerical examples based on ideal models and two practical examples in microstrip technology. Actually, this N-way dual-band power divider may be used as an N-way wideband power divider when the frequency-ratio is relatively small and can be considered as the extension of the conventional N-way Wilkinson power divider for single-band applications. The N-way (Multi-way) unequal dual-band power dividers will need in-depth study.

ACKNOWLEDGMENT

This work was supported in part by National High Technology Research and Development Program of China (863 Program, No. 2008AA01Z211), Sino-Swedish IMT-Advanced Cooperation Project (No. 2008DFA11780), and BUPT Excellent Ph.D. Students Foundation (CX200901).

REFERENCES

1. Wilkinson, E., "An N-way hybrid power divider," *IRE Trans. Microw. Theory Tech.*, Vol. 8, No. 1, 116–118, 1960.
2. Yee, H. Y., F.-C. Chang, and N. F. Audeh, "N-way TEM-mode broad-band power dividers," *IEEE Trans. Microw. Theory Tech.*, Vol. 18, No. 10, 682–688, 1970.
3. Nagai, N., E. Maekawa, and K. Ono, "New N-way hybrid power dividers," *IEEE Trans. Microw. Theory Tech.*, Vol. 25, No. 12, 1008–1012, 1977.
4. Saleh, A. A. M., "Planar electrically symmetric N-way hybrid power dividers/combiners," *IEEE Trans. Microw. Theory Tech.*, Vol. 28, No. 6, 555–563, 1980.
5. Ahn, H.-R., K. Lee, and N.-H. Myung, "General design equations of N-way arbitrary power dividers," *IEEE MTT-S International Microwave Symposium Digest*, Vol. 1, 65–68, Jun. 6–11, 2004.
6. Eccleston, K. W., "N-way microwave power divider using two-dimensional meta-materials," *Electron. Lett.*, Vol. 42, No. 15, 863–864, 2006.
7. Eccleston, K. W. and J. Zong, "Implementation of a microstrip square planar N-way metamaterial power divider," *IEEE Trans. Microw. Theory Tech.*, Vol. 57, No. 1, 189–195, 2009.
8. Rozzi, T., A. Morini, G. Venanzoni, and M. Farina, "Full-wave analysis of N-way power dividers by eigenvalue decomposition," *IEEE Trans. Microw. Theory Tech.*, Vol. 57, No. 5, 1156–1162, 2009.
9. Wu, Y. and Y. Liu, "Closed-form design method for unequal lumped-elements wilkinson power dividers," *Microwave and Optical Technology Letters*, Vol. 51, No. 5, 1320–1324, 2009.
10. Monzon, C., "A small dual-frequency transformer in two sections," *IEEE Trans. Microw. Theory Tech.*, Vol. 51, No. 4, 1157–1161, 2003.
11. Wu, Y., Y. Liu, and S. Li, "A compact Pi-structure dual band transformer," *Progress In Electromagnetics Research*, PIER 88, 121–134, 2008.
12. Wu, Y., Y. Liu, and S. Li, "A dual-frequency transformer for complex impedances with two unequal sections," *IEEE Microw. Wireless Compon. Lett.*, Vol. 19, No. 2, 77–79, 2009.
13. Wu, Y., Y. Liu, S. Li, C. Yu, and X. Liu, "A generalized dual-frequency transformer for two arbitrary complex frequency-dependent impedances," *IEEE Microw. Wireless Compon. Lett.*,

Vol. 19, No. 12, 792–794, 2009.

14. Wu, L., Z. Sun, H. Yilmaz, and M. Berroth, "A dual-frequency Wilkinson power divider," *IEEE Trans. Microw. Theory Tech.*, Vol. 54, No. 1, 278–284, 2006.
15. Cheng, K.-K. M. and C. Law, "A novel approach to the design and implementation of dual-band power divider," *IEEE Trans. Microw. Theory Tech.*, Vol. 56, No. 2, 487–492, 2008.
16. Park, M. J. and B. Lee, "A dual-band Wilkinson power divider," *IEEE Microw. Wireless Compon. Lett.*, Vol. 18, No. 2, 85–87, 2008.
17. Yang, T., J.-X. Chen, X. Y. Zhang, and Q. Xue, "A dual-band out-of-phase power divider," *IEEE Microw. Wireless Compon. Lett.*, Vol.18, No. 3, 188–190, 2008.
18. Wu, Y., Y. Liu, and X. Liu, "Dual-frequency power divider with isolation stubs," *Electron. Lett.*, Vol. 44, No. 24, 1407–1408, 2008.
19. Wu, Y., Y. Liu, and S. Li, "A new dual-frequency Wilkinson power divider," *Journal of Electromagnetic Waves and Applications*, Vol. 23, No. 4, 483–492, 2009.
20. Wu, Y., Y. Liu, and S. Li, "Dual-band modified Wilkinson power divider without transmission line stubs and reactive components," *Progress In Electromagnetics Research*, PIER 96, 9–20, 2009.
21. Wu, Y., Y. Liu, S. Li, and H. Zhou, "Compact dual-band equal power divider circuit for large frequency-ratio applications," *Journal of Infrared Millimeter and Terahertz Waves*, in press, 2009.
22. Wu, Y., Y. Liu, S. Li, and C. Yu, "A new symmetric modified Wilkinson power divider using L-type dual-band impedance matching structure," *Journal of Electromagnetic Waves and Applications*, Vol. 23, No. 17/18, 2351–2362, 2009.
23. Li, X., S.-X. Gong, L. Yang, and Y.-J. Yang, "A novel wilkinson power divider for dual-band operation," *Journal of Electromagnetic Waves and Applications*, Vol. 23, No. 2–3, 395–404, 2009.
24. Law, C. and K.-K. M. Cheng, "Compact dual-band power divider design using branch-lines and resistors only," *Asia-Pacific Microwave Conference (APMC) 2008*, 1–4, Dec. 16–20, 2008.
25. Wu, Y., H. Zhou, Y. Zhang, and Y. Liu, "An unequal Wilkinson power divider for a frequency and its first harmonic," *IEEE Microw. Wireless Compon. Lett.*, Vol. 18, No. 11, 737–739, 2008.
26. Wu, Y., Y. Liu, Y. Zhang, J. Gao, and H. Zhou, "A dual band unequal wilkinson power divider without reactive components,"

IEEE Trans. Microw. Theory Tech., Vol. 57, No. 1, 216–222, 2009.

27. Wu, Y., Y. Liu, and S. Li, "Unequal dual-frequency Wilkinson power divider including series resistor-inductor-capacitor isolation structure," *IET Microwaves, Antennas & Propagation*, Vol. 3, No. 7, 1079–1085, 2009.
28. Wu, Y., Y. Liu, and S. Li, "An unequal dual-frequency Wilkinson power divider with optional isolation structure," *Progress In Electromagnetics Research*, PIER 91, 393–411, 2009.
29. Wu, Y., Y. Liu, S. Li, and X. Liu, "A novel dual-frequency Wilkinson power divider with unequal power division," *Electromagnetics*, Vol. 29, No. 8, 627–640, 2009.
30. Wu, Y., Y. Liu, S. Li, and C. Yu, "A new design method for unequal dual-band modified Wilkinson power divider," *Electromagnetics*, accepted after revisions, 2010.
31. Feng, C., G. Zhao, X.-F. Liu, and F.-S, Zhang, "Planar three-way dual-frequency power divider," *Electron. Lett.*, Vol. 44, No. 2, 133–134, 2008.
32. Wang, W., W. Li, and D. Chen, "Design of N-way dual-frequency power divider base on genetic algorithm," *2009 International Conference on Networks Security, Wireless Communications and Trusted Computing (NSWCTC'09)*, Vol. 1, 274–277, Apr. 25–26, 2009.
33. Shamsinejad, S., M. Soleimani, and N. Komjani, "Novel miniaturized Wilkinson power divider for 3G mobile receivers," *Progress In Electromagnetics Research Letters*, Vol. 3, 9–16, 2008.
34. Oraizi, H. and M. S. Esfahlan, "Miniaturization of Wilkinson power dividers by using defected ground structures," *Progress In Electromagnetics Research Letters*, Vol. 4, 113–120, 2008.
35. Fan, F., Z.-H. Yan, and J.-B. Jiang, "Design of a novel compact power divider with harmonic suppression," *Progress In Electromagnetics Research Letters*, Vol. 5, 151–157, 2008.
36. Chang, C.-P., C.-C. Su, S.-H. Hung, Y.-H. Wang, and J.-H. Chen, "A 6 : 1 unequal wilkinson power divider with EBG CPW," *Progress In Electromagnetics Research Letters*, Vol. 8, 151–159, 2009.